

Observational Spectroscopy Lab: Detecting a spectroscopic binary

Hauer, L., Schönhacker, C., Schubert, E.

Department of Astrophysics, University of Vienna, 1180 Vienna, Türkenschanzstraße 17

12th September 2025

ABSTRACT

Aims. The goal for this observational lab is to use the spectrograph LISA to test whether it is possible to identify line splitting in the spectroscopic binary AU Ser, which has a maximum radial velocity difference between its components greater than 300 km/s.

Methods. The LISA spectrograph has a low spectral resolution of $R \approx 1000$ and covers the visual spectrum. It is used together with the telescope in the Northern Dome, *vlt*. We observe the target twice in a single night, covering both quadrature when line splitting is expected and conjunction of the binary system, when we expect no line splitting. The data is reduced using a provided pipeline, which also does the wavelength calibration of the resulting spectra. The final analyses are done using our own codes.

Results. We analyse three prominent lines in both observations and try matching them to known absorption line features. We are able to identify the Mg I b triplet, which shows a splitting of $\sim 7 \text{ \AA}$ during quadrature, which is above our detection threshold. The $H\alpha$ observed during quadrature however does not show any significant splitting. The third prominent line present in the observations can not be attributed to any absorption feature, but it also does not show any significant splitting.

Conclusions. Even if two of the three presented lines do not show splitting we hesitantly conclude that it is in fact possible to identify a spectroscopic binary using the LISA spectrograph, based on a 2σ detection of line splitting. The possibilities however are limited by LISA's spectral resolution and only possible for large radial velocities.

Key words. Observational Lab – Vienna Little Telescope – Spectroscopy – Binary stars

1. Introduction

Since the first astronomical application of spectroscopy by Fraunhofer and Kirchhoff in the early 19th century, spectroscopy has led to numerous groundbreaking advancements, including the detection of the expansion of the universe, the detection of exoplanet atmospheres and much more.¹ Nowadays spectroscopy is an essential part and many large telescopes have multiple instruments dedicated just for spectroscopy. For example, ESO's Very Large Telescope currently has eleven instruments that are capable to do some form of spectroscopy.² But also smaller observatories like the Northern Dome of the Institute for Astrophysics of the University of Vienna host spectrographs. Here in this work, we use the low resolution spectrograph LISA together with the *vlt* (Vienna Little Telescope), a modern Cassegrain reflector telescope, located in the Northern Dome of the Vienna University Observatory. It has an 80 centimetre opening and 6.64 meter focal length and is mostly used for student education.

One application of spectroscopy is radial velocity measurements to detect exoplanets. When a planet orbits a star, the star also orbits around a common centre of mass. This movement results in Doppler shifts in the host star's spectrum.³ This idea is also applicable to binary stars which are then called *spectroscopic binaries*. In this work we aim to identify this effect in the known spectroscopic binary AU Ser with the LISA spectrograph.

¹ <https://www.eso.org/public/teles-instr/technology/spectroscopy/>

² <https://www.eso.org/public/teles-instr/paranal-observatory/vlt/vlt-instr/>

³ <https://www.planetary.org/articles/color-shifting-stars-the-radial-velocity-method>

In Section 2, we will introduce the detection theory. In Section 3 the LISA spectrograph is presented. Section 4 presents the target selection process, Section 5 the data acquisition. Section 6 summarizes the data reduction and analysis. Finally, in Section 7 we present our results which are discussed in Section 8. Lastly we conclude in section 9.

2. Detection Theory

Radial velocity measurements are an often applied indirect method to detect exoplanets, but also spectroscopic binaries. Many binary stars have angular separations that are too small to resolve them individually. Then, spectroscopic observations can help to still identify them. A binary system always orbits around a common centre of mass shifting their spectra in a periodic fashion due to the Doppler effect. Measuring this effect over time allows one to construct a radial velocity curve from which orbital characteristics can be derived.

Often one of the components is significantly brighter, and when the spectrum shifts, only one spectrum is visible. This is called a *single-lined spectroscopic binary*. In other cases the components might be of the same order of brightness, and when the stellar spectra shift, both are visible. In this case, the spectroscopic binary is called *double-lined*. (Tatum 2021, p.375)

Whether we see two separate spectra depends on the orbital phase ϕ . At $\phi = 0$ and $\phi = 0.5$, both components are aligned on the line of sight and have the same radial velocity magnitude, thus the spectra overlap and we should not see any spectral line twice. At $\phi = 0.25$ and $\phi = 0.75$, the radial velocity difference between the stars is maximal and we should see spectral lines twice. This method for detecting spectroscopic binaries is not new, in fact the first spectroscopic binary ever discovered used line splitting. In

1887, Martha Hazen, a niece of the spectroscopic pioneer Henry Draper noticed splitting in the Ca K line of Mizar A at intervals of 52 days, confirming that Mizar A itself is a spectroscopic binary.⁴

3. The LISA spectrograph

The LISA spectrograph is a slit-based spectrograph with a spectral resolution of $R \approx 1000$. It covers the visual spectrum from 400 nm to 800 nm. The standard slit width used is $23 \mu\text{m}$. LISA has an integrated guiding module and thus needs two detectors, a guiding camera and an acquisition camera. (Thizy and Cochard 2012)

LISA can roughly be split into two main parts, the guiding and calibration unit and the spectrograph itself. Like in most spectrographs, the focused starlight goes through the entrance slit, is reflected by a mirror to a collimator which transforms the beam into a parallel beam. This is then diffracted by a grating and converged towards a sensor by an objective lens. LISA is illustrated in Figure 1. (Thizy and Cochard 2012)

For flat fielding, LISA uses a built-in tungsten lamp. This lamp has almost no emission or absorption lines and thus ensures an image that is as flat as possible.

Additionally, for wavelength calibration, LISA also includes a neon-argon lamp. This lamp has many known emission lines, which we can use as a reference for the wavelength calibration of our observed spectra. (Thizy and Cochard 2012)

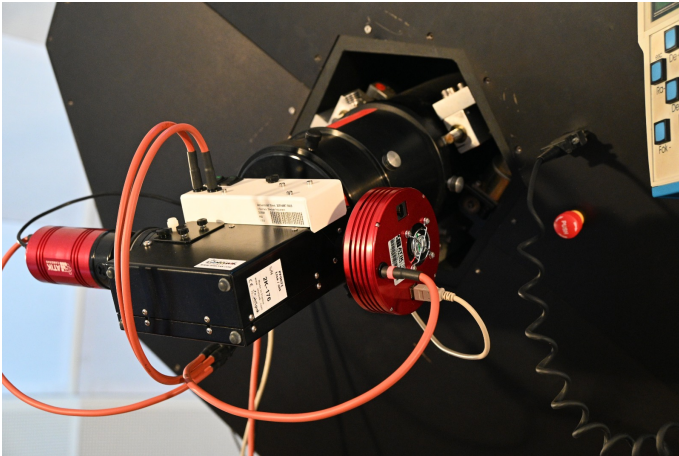


Figure 1: The LISA spectrograph mounted in the vlt.

4. Target selection

In the target selection process, we are limited by four main constraints: (1) resolving power and period; (2) limiting magnitude; (3) visibility; and (4) spectral type.

As stated before, the resolving power of LISA is roughly $R \approx 1000$. This low resolution limits the minimum radial velocity shifts we can measure to hundreds of km/s. Thus, we need a spectroscopic binary whose radial velocity amplitudes differ by at least a few hundred km/s. Also, the period of the binary should be short enough to allow frequent observational windows.

With the current setup, only targets brighter than 11 mag are feasible, as we want to keep the exposure times short.

Due to the fact that the observational spectroscopy lab is during the summer semester, we are heavily limited by the length of the

night. Also, ideally, we want the target to be at a high altitude to avoid being affected too much by the atmosphere.

Lastly, both components of the system should be A- or F-type stars, as these show the strongest hydrogen absorption lines.

Keeping all these restrictions in mind, we find the optimal target for this lab to be *AU Ser*. It is a moderately bright spectroscopic and eclipsing binary located in the constellation Serpens. According to Liu et al. (2024), it is a double-lined spectroscopic binary (SB2) and therefore fits our project. The most important stellar parameters are summarised in Table 1. The spectral type given in Table 1 is the combined spectral

Table 1: Most important stellar parameters of *AU Ser*.

^a Gaia Collaboration (2022)

^b Pribulla et al. (2009)

Type ^b	EW(A)
Spectral Type ^b	G4V
G-flux (mag) ^a	10.7 - 11.1
RA ^a	15 56 49.47
DEC ^a	+22 16 01.59
Period (d) ^a	0.386497
Epoch (JD) ^a	2457435.9954
K1 (km/s) ^b	138.77±1.33
K2 (km/s) ^b	195.64±1.34
V_0 (km/s) ^b	-61.59±0.84
ΔV_{max} (km/s)	334.41±1.90

type of the system. The fact that the system is of spectral type G conflicts with our constraints of A- to F-type stars. However, G stars still show moderate, though weaker, hydrogen lines compared to A- to F-type stars. Additionally, they show stronger metal lines. However, since other parameters of the star, like radial velocity, period and flux are significantly more favourable than those of other possible targets, we still choose *AU Ser*. Figure 2 illustrates the radial velocity curves of the components of the system, generated by the *9th Catalogue of Spectroscopic Binary Orbits*⁵. The maximum radial velocity difference between the two radial velocity semi-amplitudes K_1 and K_2 is $\Delta V_{max} = (334.41 \pm 1.90)$ km/s. This is still on the lower end of our constraint of several hundred km/s but possibly still distinguishable with LISA.

5. Data acquisition

5.1. Preparation

The observation should generally take place on a cloudless night with the relative humidity below 80-85 percent. Additionally, we are constrained by the phase of the spectroscopic binary. As stated in Table 1, it has a rather short period of ~ 0.387 days, which corresponds to ~ 9.3 hours. To show that the system is in fact a binary system, we need to observe the star conjunction and quadrature, so at $\phi = 0$ or $\phi = 0.5$ and at $\phi = 0.25$ or $\phi = 0.75$. Thus we need two observations in total, separated by ~ 2.3 hours. We can predict at which phase the binary currently is by using the fact that it is also an eclipsing binary. We can use its ephemerides measurements (epoch and period) and plug them into the relation

$$T(n) = T_0 + P n. \quad (1)$$

⁴ <https://www.leosondra.cz/en/mizar/>

⁵ <https://sb9.astro.ulb.ac.be/>

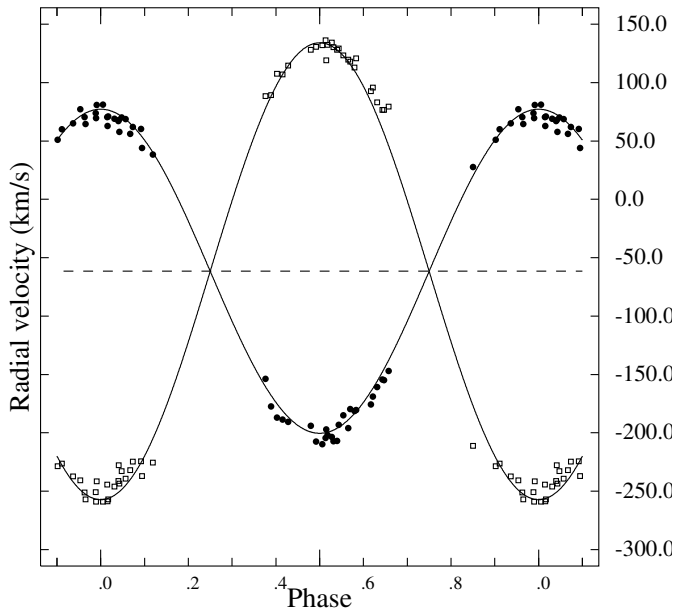


Figure 2: Radial velocity curves of AU Ser. Figure generated through the *9th Catalogue of Spectroscopic Binary Orbits*.

The epoch T_0 represents a reference minimum, P is the period and n signifies the number of the minimum we want to predict since the reference minimum T_0 . For ease, there are many websites available that predict minima based on independent observations from professionals and amateurs. One of these websites is the database *TIDAK - Timing DAtabase at Krakow*⁶ which provides O-C diagrams and future minima predictions. The database provides us with the times of primary and secondary minima which occur at $\phi = 0$ and $\phi = 0.5$. These are the times we expect no splitting of spectral lines to be visible. To now get the time when the splitting of the lines should be strongest (i.e. the phases $\phi = 0.25$ and $\phi = 0.75$), we can simply add a quarter of the period (~ 2.3 hours) to the primary and secondary minima.

After regularly checking the weather forecast, the possible observation times and the availability of the northern dome, we found that the night from 30.05.2025 to 31.05.2025 fit our constraints. We determined that the first observation should take place at 22:30 CEST. At this time, the system should be at the phase $\phi = 0.25$ and thus at its highest radial velocity amplitude difference and line splitting should be present. The second observation should take place at 00:49 CEST at the secondary minimum $\phi = 0.5$, at which we expect no splitting to be visible. In the following, we call these observations *Observation 1* and *Observation 2*.

5.2. Preparing the telescope and LISA

Before we can start observing, we first need to prepare the telescope and instrument. To do so, we check the current state of the Northern Dome. To keep the telescope dry and functional, dehumidifiers are usually active. These need to be turned off to not disturb the measurements. Next, we dismount the imaging instrument and mount LISA on the vlt. Additionally, we log into all computers and set up remote operation for convenient con-

trol from the room below the telescope. The telescope is being managed through the controller software *Autoslew*⁷. For the data acquisition we use *MaximDL*⁸, which is a useful software package for processing and analysing astronomical imaging. The next step is to open the dome. With this step one must be careful as the dome may only be opened if there is no potential danger to the telescope for example by something falling onto it. Due to this reason, the mirror of the vlt must still be covered. Only after the dome is fully opened one can remove the telescope's covers. To do so, we bring the telescope into parking position 2 and manually remove the protective cover by climbing on the blue parts of the instrument's mount as these parts are not part of the telescope itself and are therefore safe to climb on. Now we open the shutter protection of the mirror via software. Subsequently we connect both detectors of LISA to the *MaximDL* software in separate windows and turn on the camera cooling system to reduce the possible noise of the instrument.

5.3. Calibration Frames

The next step is to take the calibration frames. For the bias, we use archival data, as this type of frame does not change a lot over time. Flat frames should be taken more regularly. To create flats we turn on the tungsten lamp and take multiple frames, each well exposed, to stay in the linear region of the detector. For this, the spectrograph should already be focused. The dark frames are taken after the science observations to match their exposure times. The last calibration frame we need to take is unique to spectroscopy; the wavelength calibration files. To do so, we turn off the tungsten lamp and turn on the neon-argon lamp and again record several well exposed spectra. It is important to note that, unlike flat frames, which should be taken every observation night, wavelength calibration frames should be taken after every movement of the telescope, as even little vibrations can significantly alter how the light is dispersed on the sensor. Thus, we always take one calibration frame before starting an observation and one after finishing the observation.

5.4. Target observations

After setting up the telescope and spectrograph and taking all necessary calibration frames, we can begin with the target data acquisition. To do so, we enter the coordinates of AU Ser into the controlling software. The telescope now moves roughly to AU Ser's position. We now take one frame with the guiding camera and compare this frame to a finding chart, in our case simply with an SDSS image of our target's neighbourhood. This image can be seen in Figure 3.

⁷ <https://www.astrosysteme.com/download-center/>

⁸ <https://diffractionlimited.com/product/maxim-dl/>

⁶ astro.as.up.krakow.pl

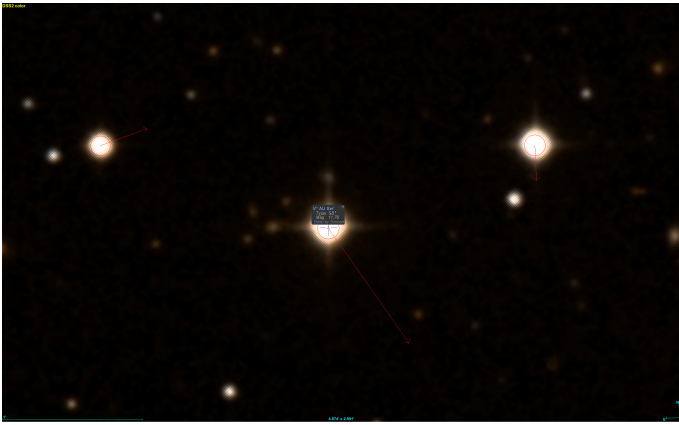


Figure 3: SDSS image of the neighbourhood of AU Ser. AU Ser is centred in the image. The FOV is roughly that of LISA/vlt.

After identifying AU Ser in the guiding camera's frame, we position it directly on the slit, like illustrated in Figure 4.



Figure 4: Test frame of the guiding camera. AU Ser is positioned directly on the slit.

Now we take test exposures with the acquisition camera to find an exposure time with enough counts. The exposure time should not be too long to be impractical and to avoid that the telescope moves too much due to inaccuracies in guiding. Some smaller guiding inaccuracies can be corrected during exposure by monitoring that AU Ser is still perfectly situated on the slit.

After this process, we wait till the determined first observation time of 22:30 CEST. Shortly before this, at 22:27, we begin acquiring spectra. In total, we take three frames, each with an exposure of 300 s. Table 2 gives an overview of all acquired frames. We stop acquiring frames 15 min after the calculated observation time. We then wait until the next calculated observation time at 00:49 CEST. Before beginning data acquisition, we again position the star perfectly on the slit. We again take three exposures, each 300 s long. We stop acquisition 19 min after the calculated time.

Table 2: Observation and calibration overview.

Observation 1	Time/Amount	Exposure time
Calculated time	22:30 CEST	
Science frames	3	300 s each
Reference frames	2	180 s each
Observation 2	Time/Amount	Exposure time
Calculated time	00:49 CEST	
Science frames	3	300 s each
Reference frames	2	180 s each
Calibration	Amount	Exposure time
Dark frames	2	300 s each
Flat frames	2	15 s each

5.5. End procedure

Before finishing the observation we need to take dark frames that match the exposure times of our science frames. For taking the dark frames, we close the shutter so that no photons can hit the sensor of our acquisition CCD. In total we take 2 darks, each with an exposure of 300 s.

As the data is now gathered and the observation is over, we start with the post-observational procedure. First of all, we run the "Warm up" command in the camera software. Then we close the mirror shutter via *Autoslew* "Close Mirror Covers". In order to put the cover foils on, we park the telescope back into park position 2 and manually put them on. Then we proceed with closing the dome shutter facing East and parking the telescope in park position 1. Now the softwares can be closed and the air dehumidifier turned on. We disconnect LISA from the electricity, log out of the computer and log our observations in the logbook.

6. Data reduction and analysis

For data reduction and analysis, we use a pipeline made available to us by Heinz Weber. In the following, we quickly summarise the most important aspects.

The pipeline can be separated into four main parts: (1) data reduction, (2) geometry, (3) spectral calibration and (4) analysis. Spectroscopic data reduction is similar to normal CCD reduction. The pipeline already comes with archival darks for the wavelength calibration frames and with archival bias frames. The only thing the software still needs for part 1 are the flat frames, dark frames for the science exposures, calibration frames and science frames taken during the observation. The software now automatically creates master files and does the appropriate bias, dark and flat correction for both the science exposures and the wavelength calibration files according to the standard scheme. It then stacks the science files for an improved SNR.

In part 2, the pipeline corrects the spectrum for the tilting effect present in every spectrum taken with LISA. After this, it also cuts out the spectra.

Next, part 3 measures both the science and reference spectra by averaging along their dispersion direction. The reference spectrum is then fitted with the known emission lines of the neon-argon lamp. This results in a wavelength calibration model, which can be applied to the science spectrum. In part 4 of the pipeline, emission and absorption lines are detected in the spectrum. In this work we however use our own analysis methods, explained in the following.

After using the pipeline for both observations, we begin our own data analysis procedure. We plot the calibrated spectra

from Observation 1 and observation 2 in the same plot to compare them better. Next, we smooth both spectra with a *Savitzky-Golay Spectral Filter* implemented in the *scipy.signal* package. This type of filter is often used to smooth spectra, while still retaining the shape of a peak.⁹ From this we can estimate the continuum, which is used to divide the total signal of both observations. The results is flattened spectra, which are easier to analyse.

Overly noisy data at the edges of the spectra – below 4000 Å and above 7600 Å – is masked. We then plot vertical lines at the wavelengths of the most prominent absorption features and compare them to literature values, to identify the element.

Both spectra are visually compared around these wavelengths to search for line broadening, or even a clear splitting of spectral features. To assess whether apparent splitting could simply be due to noise, we use the Doppler shift relation

$$\Delta\lambda = \lambda \frac{\Delta v}{c}. \quad (2)$$

By inserting the maximum radial velocity difference between the two components, ΔV_{\max} , we obtain the expected wavelength shift for each star, and thus the total separation (or “splitting”) between the two components of a spectral line. For instance, the expected splitting for the $H\alpha$ line at 6562.8 Å is approximately 7.32 Å. At 5000 Å the separation decreases to about 5.58 Å, and at 4000 Å to about 4.46 Å.

Assuming that the spectrograph LISA provides a constant resolving power of $R \sim 1000$, we can estimate the instrumental resolution element,

$$\Delta\lambda_{\text{ins}} = \frac{\lambda}{R}, \quad (3)$$

which gives the smallest wavelength difference that can be resolved. Table 3 summarises a comparison between the theoretical resolution limit of LISA and the predicted line splitting at several diagnostic spectral features, that might be found in a typical stellar spectrum.

Line	WL (Å)	$\Delta\lambda_{\text{ins}}$ (Å)	Predicted splitting (Å)
Na doublet	~8592	8.59	9.59
O triplet	~7774	7.77	8.67
TiO	7589.00	7.59	8.46
TiO	7053.00	7.05	7.87
$H\alpha$	6562.81	6.56	7.32
Mg b triplet	~5172	5.17	5.77
$H\beta$	4861.34	4.86	5.42
$H\gamma$	4340.47	4.34	4.84
$H\delta$	4101.74	4.10	4.57

Table 3: Comparison between the theoretical resolution limit of LISA ($R \sim 1000$) and the predicted splitting of selected spectral lines.

Additionally, we also assess the noise of the flux to determine the significance of detections we may find. We do so by first subtracting the continuum from the spectra to get the residuals. We then apply sigma clipping to the residuals to mask spectral lines. We then determine the noise of the spectra by calculating the standard deviation of the masked residuals.

⁹ http://www.dmscripting.com/savitzky-golay_spectral_filter.html

7. Results

Figure 5 shows the calibrated spectrum of Observation 1 after using the pipeline by Heinz Weber.

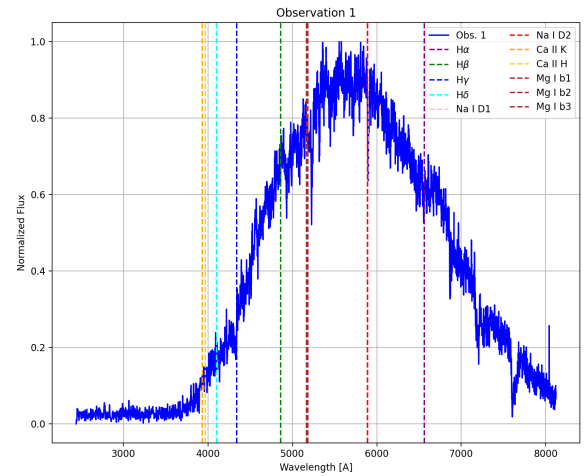


Figure 5: Calibrated spectrum of Observation 1. The most prominent absorption lines in a usual stellar spectrum are marked with vertical dashed lines for analysis.

The result of applying a Savitzky-Golay Spectral Filter to subtract the stellar continuum is illustrated in Figure 6.

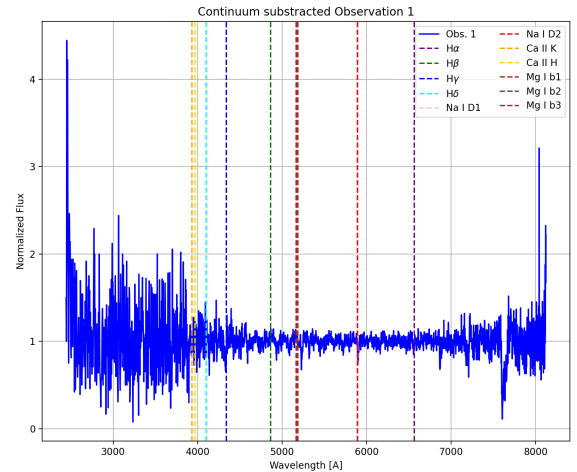


Figure 6: Continuum-subtracted spectrum of Observation 1. The most prominent absorption lines in a usual stellar spectrum are marked with vertical dashed lines for analysis.

As visible in Figure 6, at the edges, the spectrum is noisy. Thus we mask the overly noisy data below 4000 Å and above 7600 Å. We find for both masked observations that the standard deviation, and thus an estimate of the noise of our data, is

$$\sigma_1 \approx 0.035 \text{ ADU}, \quad (4)$$

excluding spectral lines through sigma clipping. Thus, every change in flux we find above this threshold could be attributed to

a real physical measurement.

We visually inspect and fit all strong absorption lines in both observations with a Gaussian fit. We assess if the lines show either broadening and/or splitting in Observation 1. In the following, we present three representative lines for the whole spectrum.

The first absorption line feature we present is, as we believe, the *Mg I b* triplet. It originates at wavelengths of 5183 Å, 5172 Å and 5167 Å, although the last two cannot be distinguished from each other with LISA, as their separation is below the theoretical resolution limit. Figure 7 shows the two spectra, Observation 1 and Observation 2 being coloured blue and orange respectively. It is apparent that we see a splitting of one of the *Mg I b* lines during Observation 1, which is not present in Observation 2. To better analyse the lines, we fit Gaussian profiles to them (dashed yellow and black lines for Observation 1; dashed red line for Observation 2). Table 4 illustrates the results of the fits and shows, that there is a mismatch between theoretical wavelengths and the measured wavelengths of the lines (more on that in Chapter 8). The amount of splitting in Observation 1 is ~ 7.1 Å, which is significantly larger than the resolving limit. The depth of the absorption line is roughly twice the noise of the spectrum. At ~ 5242 Å a second line of the triplet can be seen in both spectra. Observation 2 shows a significantly larger depth than Observation 1. However, no splitting is apparent in this line.

Table 4: Results from the Gauss fits to the *Mg I b* lines

	Measured WL (Å)	FWHM (Å)
Observation 1	5227.2 & 5234.3	7.1 & 2.8
Observation 2	5229.8	8.5

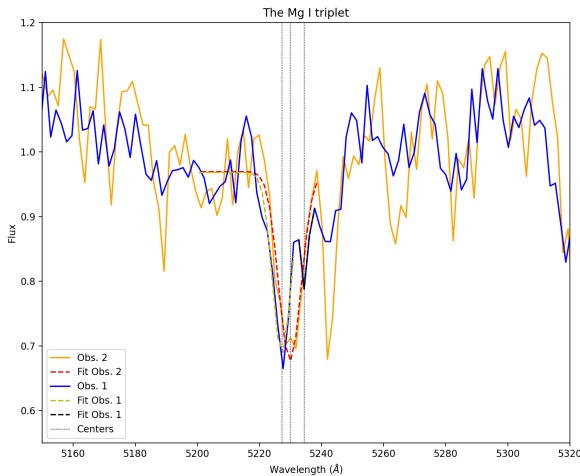


Figure 7: The *Mg I b* triplet in Observation 1 (blue) and Observation 2 (orange). The dashed lines illustrate the Gaussian fits to the spectral lines. The thin black dashed lines mark the centres of the lines determined by the fits.

The second line we present is the $H\alpha$ line normally found at 6562.8 Å. Figure 8 illustrates this line and the Gaussian fits. No splitting is visible. The centres of the $H\alpha$ line in both observations lie at 6556.1 Å, so they are ~ 7 Å off. The FWHM of the

line for Observation 1 and Observation 2 are 5.5 Å and 4.8 Å respectively.

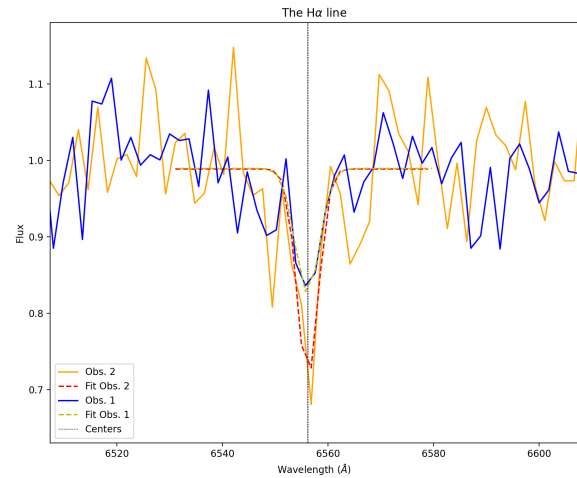


Figure 8: The $H\alpha$ line in Observation 1 (blue) and Observation 2 (orange). The dashed lines illustrate the Gaussian fits to the spectral line. The thin black dashed line marks the centre determined by the Gaussian fits.

It was not possible to identify the last line we present here (Figure 9), even though the line is strong. This is because no known absorption line is close to the central wavelengths determined by the Gaussian fits. We find that for Observation 1, the central wavelength of the line is 6868.1 Å and has a FWHM of 9.2 Å. The fit for Observation 2 results in a central wavelength of 6870.4 Å and a FWHM of 8.3 Å. Even though visually we see splitting in both lines, this has to be attributed to noise as it is below our resolution limit.

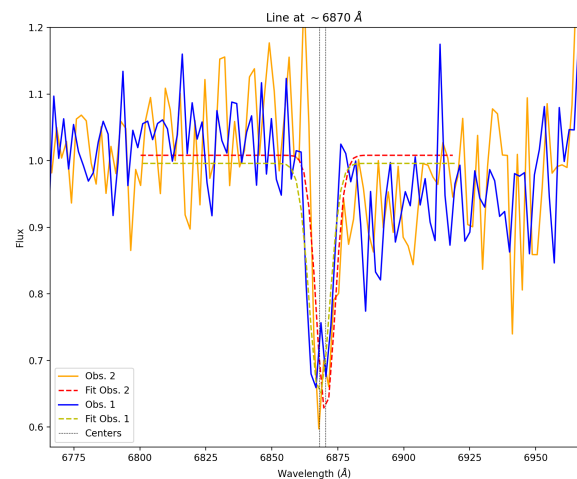


Figure 9: Unknown strong absorption line at ~ 6870 Å. Observation 1 is blue and Observation 2 in orange. The dashed lines illustrate the Gaussian fits to the spectral line. The thin black dashed lines mark the centres determined by the Gaussian fits.

8. Discussion

During analysis, we noticed that prominent absorption features like the $H\alpha$ line and the Mg I b triplet seem to be noticeably off their laboratory wavelength. We find $H\alpha$ to be $\sim 7 \text{ \AA}$ off, the Mg I b triplet even 60 \AA . This effect is so large that it cannot be attributed to Doppler shifting, which is at most 1 \AA . Thus we suspect that there might be problems with the wavelength calibration of the spectrum.

Analysing the calibrated reference spectrum, we notice that the wavelengths of the most prominent emission lines do not match with the reference wavelengths provided in the pipeline. Thus we can conclude that there is a problem with calibrating the reference spectrum, which leads to a wrong calibration of our observations. We are unsure why the calibration of the reference is wrong, although we notice that the error is not the same for every wavelength. Although a wrong wavelength calibration is displeasing, we argue that it should not interfere with our project, as we only aim to observe line splitting. However, due to this, we give no error estimates for determined line centres, as they are wrong in any case.

In Section 7 we presented three absorption features that are representative of our results, but we also analysed absorption lines beyond those three, in both observations. We only find line splitting in the absorption features which we attribute to the Mg I b triplet (Figure 7). Even though the feature is a triplet, we are only able to see two lines, as our spectral resolution is not large enough to resolve two of them independently. In Observation 1 in Figure 7, a clear splitting in the line is visible. The amount of splitting is $\sim 7.1 \text{ \AA}$, which is a bit more than the 5.77 \AA we predict and also more than our theoretical limit. The depth of the spectral line is around twice the noise of our spectrum.

We also observe splitting in both observations of an unknown line, illustrated in Figure 9. However, here the amount of splitting is little more than 3 \AA , so significantly below the resolution limit. Even though the depth of the split is also twice the noise of the spectrum, we can thus discard the splitting as noise. Additionally, we mention that our noise estimate is for the whole spectrum. Even though we have masked the overly noisy edges, the outer parts of the spectra are still significantly more noisy than in the centre. As this unknown line is more towards the red part of the spectrum, the noise is in reality significantly larger than our estimate and thus the depth of the line is not twice the noise.

The third line we present is the $H\alpha$. We detect it $\sim 7 \text{ \AA}$ off its laboratory wavelength. The line is not split. As it is the case with the unknown line, the FWHM measured by a Gaussian fit is a little larger for Observation 1 than for Observation 2. We notice this trend in every line we analyse, except for the split line in Figure 7, where we treat Observation 1 as two individual lines. We attribute this observation of larger FWHMs in Observation 1 to the same effect that causes the line splitting, just that we can't resolve the splitting, as the lines are intrinsically broad. Thus we only see a partial overlapping of the lines, producing broader features.

To summarize, for Observation 1 we only see splitting that cannot be explained by noise in one line, which we believe to be one of the Mg I b triplet lines. For Observation 2, where we do not expect splitting, we do not identify any splitting above the noise and resolution limit. In Observation 1, we find broader lines than in Observation 2. Due to all this we tentatively confirm that AU Ser is a double-lined spectroscopic binary

system, even though only one line shows splitting. However, this detection is only 2σ , leaving large room for uncertainties. Of course, we have picked the target AU Ser to be a double-lined spectroscopic binary according to Liu et al. (2024) to try to illustrate this method with LISA. In fact, AU Ser was found to be a double-lined spectroscopic binary using observations from the *LAMOST* low-resolution survey with a spectral resolution of $R \sim 1800$, not much more than LISA.

9. Conclusion

We tentatively confirm that we can apply the method of line splitting to observations with LISA, in order to detect spectroscopic binaries. We apply this method to the known double-lined spectroscopic binary AU Ser with a maximum radial velocities difference between both components of more than 300 km/s . We observe AU Ser twice, once at quadrature (Observation 1) when we expect maximum line splitting and once at conjunction (Observation 2), when we expect no splitting. Out of several spectral lines, we can only report a 2σ detection for one spectral line in Observation 1. Additionally to the splitting, Observation 1 shows broader spectral lines than Observation 2, which we attribute to the same effect that causes the splitting. Observation 2 shows as expected no splitting.

References

- Gaia Collaboration. VizieR Online Data Catalog: Gaia DR3 Part 4. Variability (Gaia Collaboration, 2022). VizieR On-line Data Catalog: I/358. Originally published in: 2023A&A...674A...1G, May 2022.
- J. Liu, B. Zhang, J. Wu, and Y.-S. Ting. Double-lined spectroscopic binaries from the lamost low-resolution survey. *The Astrophysical Journal Supplement Series*, 275(2):40, nov 2024. . URL <https://dx.doi.org/10.3847/1538-4365/ad856a>.
- T. Pribulla, S. M. Rucinski, H. DeBond, A. De Ridder, T. Karmo, J. R. Thomson, B. Croll, W. Ogłóza, B. Pilecki, and M. Siwak. Radial Velocity Studies of Close Binary Stars. XIV. *AJ*, 137(3):3646–3654, Mar. 2009. .
- J. Tatum. *Celestial Mechanics*. LibreTexts, 2021. URL <https://books.google.at/books?id=jUJh0AEACAAJ>.
- O. Thizy and F. Cochard. Lisa pack: High luminosity spectrograph user guide and refernece manula, 2012.